Non-destructive Observation of Laminate Pouch Bonding Quality by Dynamic Heat Conduction Following Flash Heating

Minoru Aoyagi[*1], Takefumi Hiraguri[2], Takahiro Ueno[3]

Electrical and Electronics Engineering, Nippon Institute of Technology
4-1 Gakuendai, Miyashiro, 345-8501 Saitama, Japan
[*1]aoyagi@nit.ac.jp; [2]hira@nit.ac.jp; [3]ueno@nit.ac.jp

Abstract- **Lamination is an effective way to protect and preserve materials from destruction or deterioration. In this paper, a method for determining the quality of bonding between a laminate pouch film and paper is described. In this method, rapid heating of the surface of the laminate film bonded to paper by a light flash was followed by thermographic observation of the dynamic changes in surface temperature. The method exploits the differences in dynamic heat transport caused by poor bonding between the laminate and the paper. We carried out verification experiments on test pieces constructed to simulate poor bonding and found that the temperatures in regions of poor bonding were lower compared to regions of good bonding. Here, we outline the theoretical basis of the detection of the poor bonding, and also describe different types of insufficient bonding characterized by a temperature higher than the surrounding material. Finally, we discuss the applications and limitations of the observation method.**

Keywords- Laminate Pouch Film; Poor Bonding Detection; Thermography; Non-destructive Testing

I. INTRODUCTION

Laminating is the process of bonding a thin transparent plastic film to the surface of materials such as paper, plywood, or glass [1-3]. Lamination can increase the durability of an item as well as enhance properties such as transparency and aesthetic quality. The process of laminating is quite simple and is carried out in one of two ways: roll lamination or pouch lamination. Roll laminating machines are typically used for commercial scale applications, and pouch laminating machines are used in the home and office. Examples of laminated items include business cards, certificates, restaurant menus, leaflets, tags, photos, and other printed items. Pouch lamination is carried out by using a hot laminating film, which is usually sealed on one side. The inside of the pouch is coated with a heat-activated adhesive film that binds to the surface of the item in the laminator as the pouch passes through a set of heated rollers. Poor bonding between the laminate film and the surface of the item can decrease transparency and lead to item degradation, which in turn leads to poor long-term protection.

Steady-state thermography is a non-destructive testing method that is well-known in industrial, medical and building fields [4-17]. In dynamic thermography, a short pulse of energy is used to raise the temperature of the target material and the ensuing dynamic temperature changes are monitored. Typical pulsed energy sources include ultrasonic oscillation [18], lasers [19, 20], eddy currents [21], and light flashes [22]. Researchers have been investigating a defect observation method that utilizes dynamic infrared thermography for the detection of poor-quality bonding in the lamination of wood panels with materials such as decor films, high-pressure decorative laminate (HPL), and melamine [23-28]. However, the principles behind the detection are not yet fully known, and few reports have clarified the detection of poor-quality bonding between the laminate film and paper. In this paper, we describe the detection method for determining insufficient bonding between laminate film and paper. This is achieved by using high-speed high-performance thermography to observe the rapid changes in temperature that occur on the surface of a laminate film following heating by a light flash.

The paper is organized as follows. In Section II, the experimental setup and procedure are described. In Section III, experimental results for the detection of poor laminate bonding are presented. In Section IV, an analysis of the results and a description of the detection principle are discussed. Finally, conclusions are presented in Section V.

II. OBSERVATION SETUP AND EXPERIMENTAL PROCEDURE

The experimental setup for determining poor bonding is shown in Fig. 1(a). The setup consists of an InfReC Thermography R300 infrared camera (NEC Avio Infrared Technologies Co. Ltd.), a Xenon flash lamp (Digital studio flash CD-1200, Ningbo Suncy Electric Appliance Co., Ltd.), and a system control computer. The infrared detector consists of 320 (horizontal) × 240 (vertical) arrays of microbolometers with a detection wavelength range from 8 to 14 μm, and a temperature resolution of 0.05 ℃ at 30 ℃ with ±1 ℃ precision. The thermography transmits two-dimensional temperature data to the control computer at 60 Hz. The temperature was recorded for 50 seconds just before the light flash. The Xenon flash is used for transient heating of a test piece. The lamp spectrum, flash energy and lighting time of the flash all affect the temperature of the target material. The 16.8 mF capacitors, charged to 326 V, supply 893 J per flash. The lamp spectrum, shown in Fig. 1(b), ranges from 200 to 900 nm and is recorded by a USB2000+ spectrometer (Ocean Optics Inc.). We could not measure the spectrum over 900 nm. In general, the emission intensity of the Xenon flash over 900 nm is less than the intensity at approximately 890 nm, and in particular, the intensity over 2 μm is very low [29-31]. A photodiode (S9648, Hamamatsu Photonics K. K.) is used to measure the pulse duration, as shown in Fig. 1(c). The flash is depleted within 41 ms at a peak level of 50%. The radiation energy and time, which were the characteristic values of the flash lamp device, were not changed throughout the experiment. The position of the equipment in the experimental setup shown in Fig. 1(a) was optimized through preliminary experiments to yield the clearest indication of poor laminate bonding, and was fixed throughout the experiment.

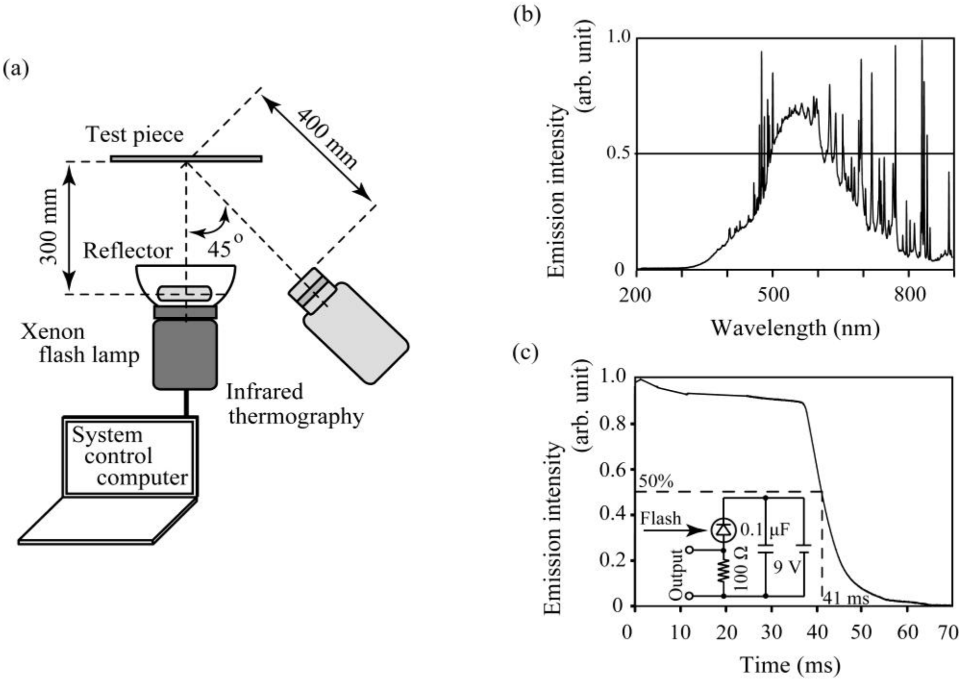

Fig. 1 (a) Schematic of the observation system. (b) Relative spectral characteristics of the flash. (c) Lighting time of the flash, measured using the circuit shown inside the plot. Temperature was recorded for 50 seconds from just before the light flash. The position of the equipment in the experimental setup shown in Fig. 1(a) was optimized through many preliminary experiments to yield the clearest indication of poor laminate bonding, and was fixed throughout the experiment.

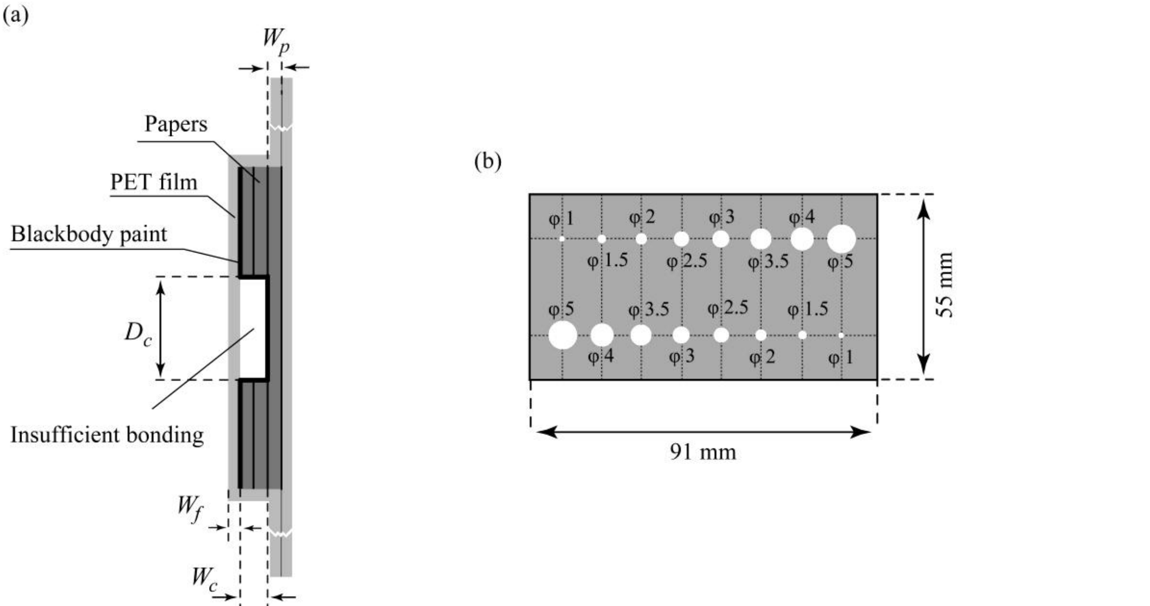

Fig. 2 Schematic diagram of the test piece, where the cavity diameter is D_c, the distance between the paper module and the laminate film within the cavity is W_c, the laminate film thickness is W_f, and the thickness of the paper is W_p. (a) Cross-sectional structure of the test piece. (b) Front view of the paper module.

Reliable reproducing of poor lamination bonding in real applications is difficult, so experiments were conducted using purpose-built test pieces. The construction of a test piece is shown in Fig. 2(a). The center of the test piece is a cylindrical cavity. The cavity is created by stacked white paper sheets with the appropriate section removed, and it is assumed to be air-filled. Laminate covers the top sheet of paper, but does not fill the cavity. Hence, the cavity simulates a region of poor laminate bonding. The diameter of the cavity, denoted by D_c, can be changed by altering the size of the hole cut in the paper. The distance between the paper and the laminate film within the cavity is denoted by W_c, the thickness of the laminate film by W_f, and the thickness of the paper by W_p. The size of a single sheet of paper is 91 mm (width) × 55 mm (height) × 0.23 mm (thickness). Therefore, W_c was 0.23 mm, 0.46 mm or 0.69 mm, determined by adding additional sheets of paper to the stack. The stacked papers are referred to as the paper module. Cavities with different diameters could be situated on one shared module, as shown in Fig. 2(b). To ensure the temperature measurement of the cavity, two sets of cavities with the same diameters were arranged on one paper module. The paper module surface was coated with blackbody paint (emissivity 0.94) to improve flash absorption and the accuracy of temperature measurements. All temperature data shown in this paper were converted by the emissivity 0.94.

The laminate film used in this work consists of a three-layered film structure of poly-ethylene-terephthalate (PET)/low-density poly-ethylene (LDPE)/ethylene-vinyl acetate copolymer (EVA). The PET is the base material. The EVA acts as glue with a low melting point (72 ℃ to 102 ℃). The LDPE film melts at a higher temperature (120 ℃ to 160 ℃) and improves the bonding between the laminate film and paper. LDPE and EVA change from opaque to transparent when heated. The laminate film thicknesses used were 0.07, 0.09, 0.17, and 0.24 mm and the laminate films were pouched at 140 ℃ by the laminator.

III. EXPERIMENTAL RESULTS

Figure 3(a) shows the two-dimensional temperature distribution on the surface of a test piece (W_f = 0.07 mm, W_c = 0.23 mm), as measured by the imaging system shown in Fig. 1(a). The distribution was recorded 0.5 s after the maximum surface temperature was reached following flash heating. The temperature profiles, which show the temperature change resulting from the flash, measured along the dashed line in Fig. 3(a), are shown in Figs. 3(b) to 3(d) for varying laminate thicknesses. The times shown in Figs. 3(b) to 3(d) are times elapsed since the maximum surface temperature was reached. The laminate thickness values in the figures were 0.07, 0.17, and 0.24 mm, respectively, and W_c was fixed at 0.23 mm. As shown by the dark color in Fig. 3(a), the temperature of the test piece was higher than the ambient temperature. Furthermore, the temperatures in regions of simulated poor bonding were lower than the rest of the test piece. The detection system could detect the simulated poor bonding of gap thickness (W_c) 0.23 mm regardless of the thickness of the film W_f (0.07 mm < W_f < 0.24 mm). The diameters of the cavities are small, so the temperature differences between the cavities and the surrounding laminate film are also small. The thicker laminate films show a lower rise in temperature than the thinner films. The high-temperature regions cool to the ambient temperature within several seconds, resulting in a uniform surface temperature.

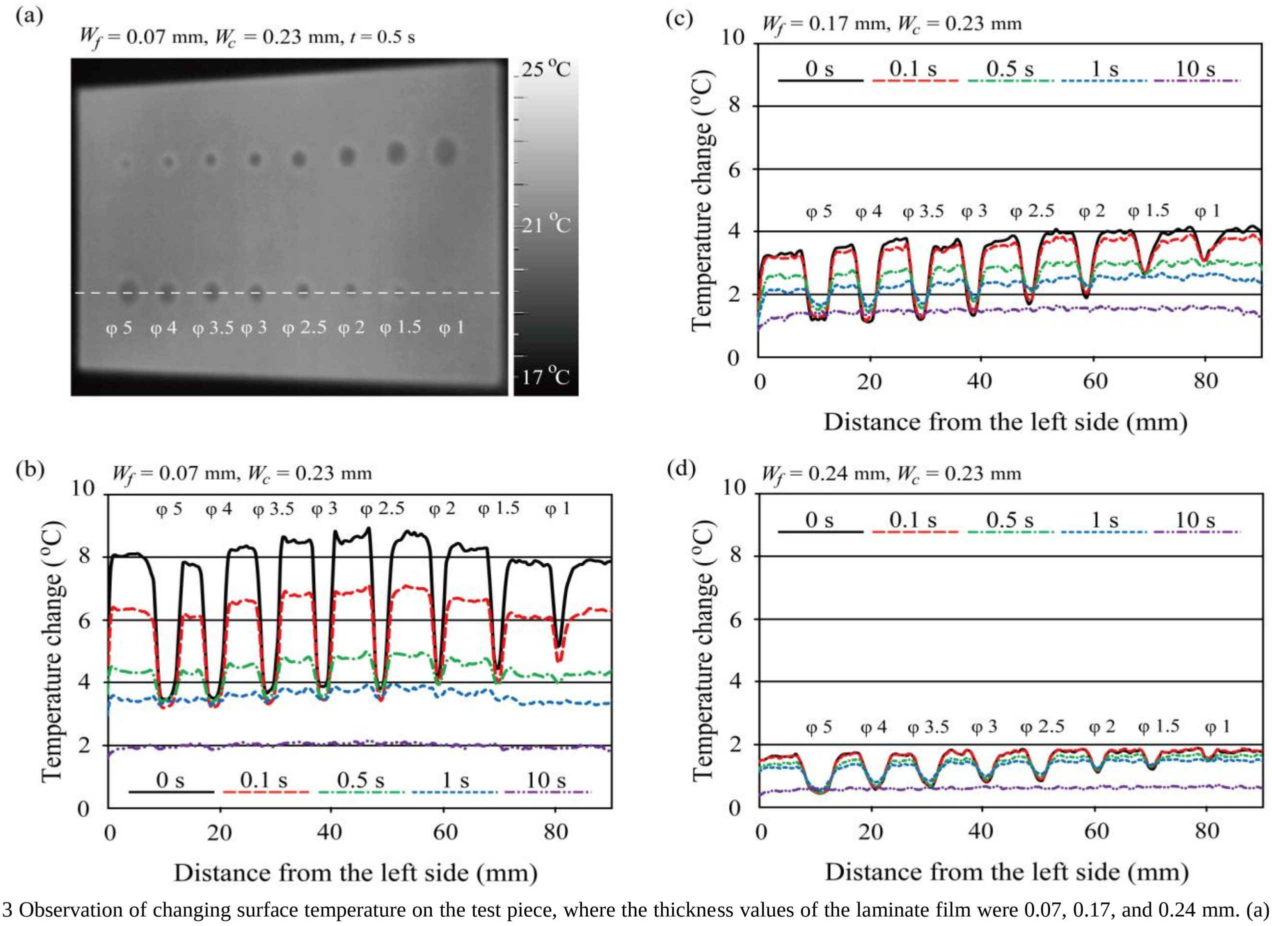

Fig. 3 Observation of changing surface temperature on the test piece, where the thickness values of the laminate film were 0.07, 0.17, and 0.24 mm. (a) Two-dimensional temperature distributions, which were recorded 0.5 s after the maximum surface temperature was reached. (b) to (d) Temperature change resulting from the flash, measured along the dashed line in Fig. 3(a). Times shown in Figs. 3(b) to 3(d) are times elapsed since the maximum surface temperature was reached.

Figure 4(a) shows the two-dimensional temperature distribution on the surface of another test piece (W_f = 0.09 mm, W_c = 0.23 mm), also recorded 0.5 s after the maximum surface temperature was reached. The temperature profiles, which show the temperature change resulting from the flash, measured along the dashed line in Fig. 4(a), are shown in Figs. 4(b) to 4(d). The times shown in Figs. 4(b) to 4(d) are times elapsed since the maximum surface temperature was reached. The temperature profiles in Figs. 4(b) to 4(d) were obtained for varying gap thicknesses. Again, it is apparent that the temperature of the test piece was higher than the ambient temperature, and that the temperatures in the regions of simulated poor bonding were lower than the rest of the test piece. Gap thicknesses W_c for these figures were 0.23, 0.46, and 0.69 mm, respectively, and the laminate thickness W_f was 0.09 mm. The detection system could detect the simulated poor bonding of film 0.09 mm in thickness regardless of the gap thickness W_c (0.23 mm < W_c < 0.69 mm). The temperatures in the cavity portions are slightly reduced as the gap thicknesses increase. This reduction is presumably caused by the attenuation of the flash by the increasing gap thickness, or optical path length.

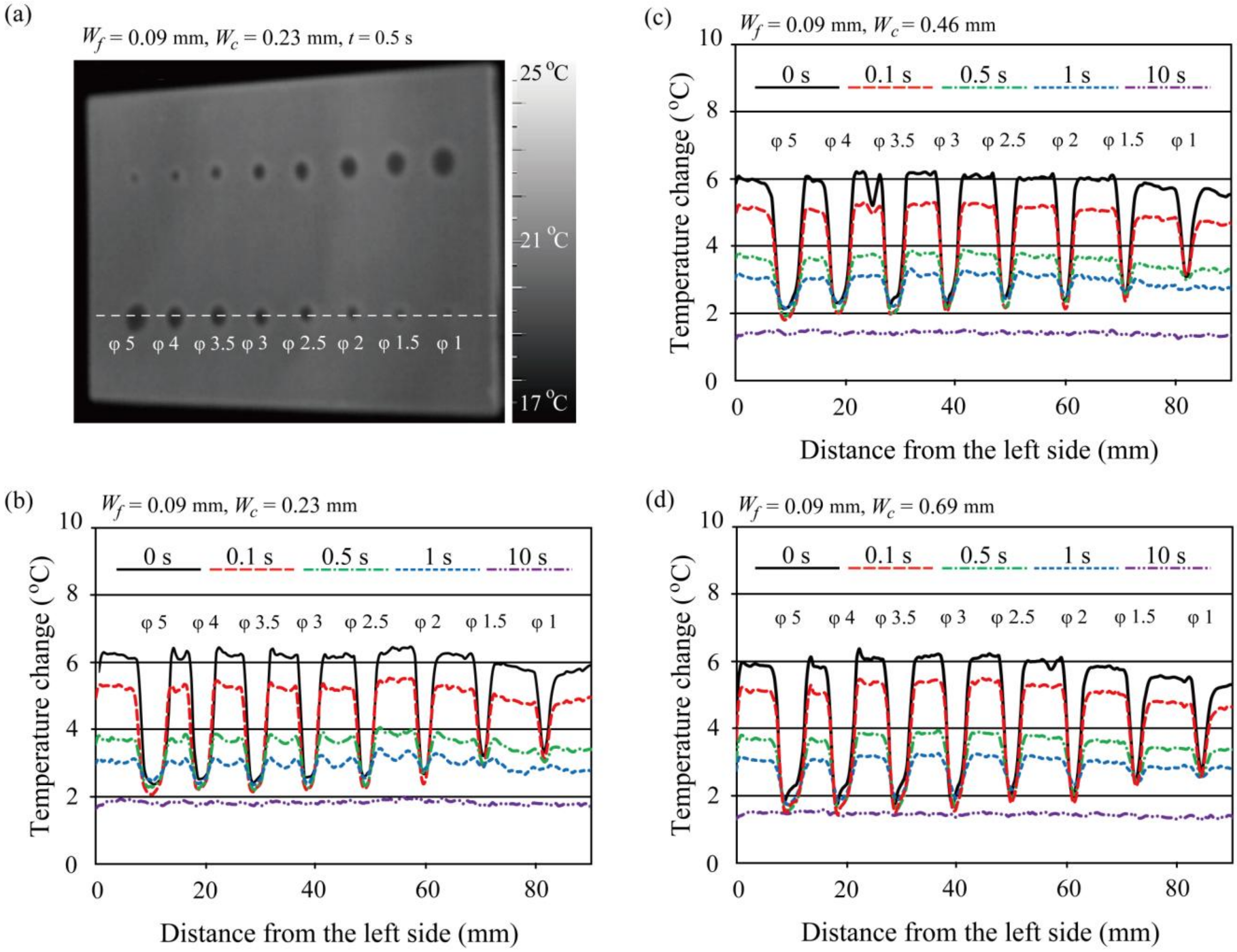

Fig. 4 Observation of changing surface temperature on the test piece, where the gap thicknesses W_c were 0.23, 0.46, and 0.69 mm. (a) Two-dimensional temperature distributions, which were recorded 0.5 s after the maximum surface temperature was reached. (b) to (d) Temperature change resulting from the flash, measured along the dashed line in Fig. 4(a). Times shown in Figs. 4(b) to 4(d) are times elapsed since the maximum surface temperature was reached.

IV. DISCUSSION

A. Analysis of Low Temperature at Regions of Poor Bonding

Infrared transmittance spectra of the laminate films used in the test pieces are shown in Fig. 5(a). The spectra were recorded by an FT/IR-4200 spectrometer (JASCO Corporation). The transmittance spectra were collected for two sheets laminated together with no material contained within. Therefore, the transmittance of single laminate sheets is the square root of the raw transmittance spectra data recorded by the spectrometer. The transmittance spectra shown in Fig. 5(a) were subjected to such calculations. We could not measure a transmittance spectrum of less than 1.3 μm. However, the film is transparent in appearance, and in general, the transmittance spectrum of the PET film in the visible light region maintains the transmittance at approximately 1 μm [32, 33]. In Fig. 5(a), the laminate films transmit light of less than 2 μm regardless of thickness, and light of more than 2 μm attenuates as the film thickness increases. Figure 5(b) shows the temperature change from the flash on the surface of the test piece that was obtained by bonding the laminate film to a single sheet of paper (W_p = 0.23 mm) without cavities and coated with blackbody paint. The thicker laminate films show a lower rise in temperature than do the thinner films. Namely, regardless of the thickness of the film, the laminate films transmit the flash, of which the main component is visible light. However, in comparison with the thin films, the thick films attenuate the infrared of more than 2 μm emitted from the test piece heated by the flash. As a result, the thick laminate films show a lower rise in temperature, as seen in Fig. 3, because the detection wavelength range of the thermography is from 8 to 14 μm.

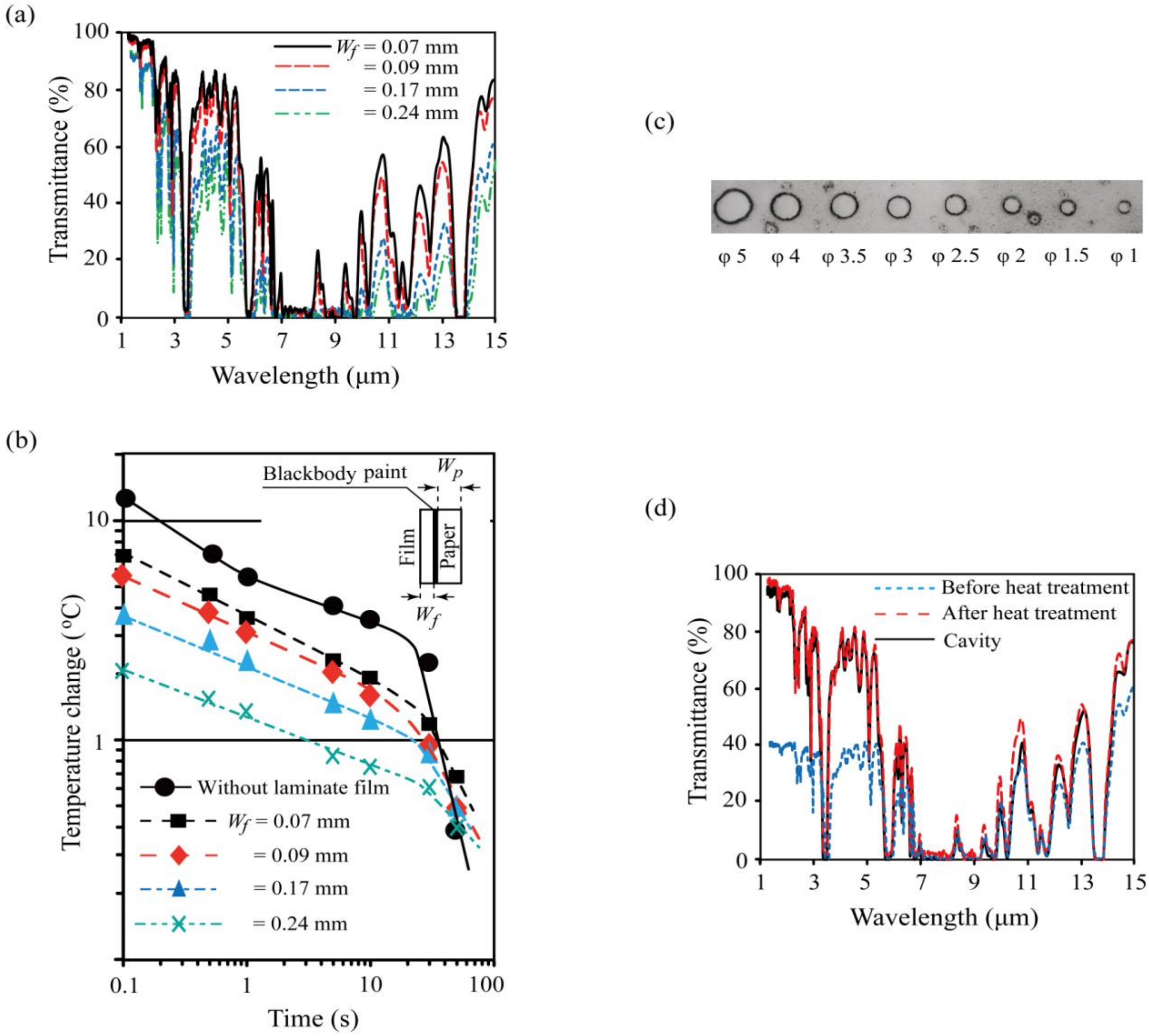

Fig. 5 (a) Transmittance spectra of the laminate films, where the film thickness values were 0, 0.07, 0.09, 0.17, and 0.24 mm. (b) Temperature changes on the surface of the test piece. (c) A photograph of the laminate film peeled off from a paper module. (d) The transmittance at the cavity, and the laminate films before and after heating.

A photograph of the laminate film (thickness 0.09 mm, gap thickness 0.23 mm) peeled off the paper module is shown in Fig. 5(c). The transparency makes a little difference in the cavity parts and other parts. To check the film transparency, the transmittance spectrum was recorded for the central portion of the film covering the cavity, as shown in Fig. 5(d); in addition, transmittance spectra before and after heat treatment of the film (that is, before and after going through the laminator with built-in heated rollers) are also shown in Fig. 5(d). The transmittance of the film before heat treatment is very low for wavelengths of less than 2 μm, but then it changes from opaque to transparent after heated by the laminator. It is considered that the light transmittance of the film in the case of good bonding equals the light transmittance of the film after heat treatment. The transmittance of the film covering the cavity is lower than the transmittance of the laminate after heat treatment and is higher than the transmittance of the laminate before heat treatment. Namely, the causes of the cavity temperature becoming lower than the temperature in other areas are as follows. First, the flash that irradiates the cavities is slightly attenuated by the film covering the cavity. Second, the infrared in the wavelength range emitted from the cavity is 8 to 14 μm, which is the detection wavelength range of the thermography and is attenuated by the film covering the cavity. Therefore, poor laminate bonding, as simulated by the cavity, can lead to lower observed temperatures.

It may be possible to consider the detection principle of simulated poor bonding as a thermal circuit consisting of thermal conduction and thermal radiation from the blackbody paint, in which the flash heat is stored. However, the radiation heat transfer from the blackbody paint to the thermography through the transparent pouch film is difficult to model as a thermal circuit using practical radiation resistances, so the thermal circuit was not considered in this work.

As shown in the temperature deviation profiles in Figs. 3 and 4, the difference in temperature between the cavities and the rest of the test pieces decreases with cavity diameter. This is due to the spatial resolution of the thermography (0.48 mm with the equipment positioned in this experimental setup). When the size of the cavity becomes the same with the spatial resolution, the temperature of the hole cannot be differentiated to the temperature of its surroundings.

B. Other Types of Insufficient Bonding

A new test piece was constructed and laminated with an uneven surface and no cavities, as illustrated in Fig. 6(a). Papers of thickness 0.23 mm were piled sporadically in different areas of the test piece, and the module was coated with blackbody paint. A two-dimensional temperature distribution obtained 0.1 s after flash heating is shown in Fig. 6(b). Higher-temperature portions in the distribution were checked for poor bonding by visual inspection. Upon peeling the laminate film off the paper module, blackbody paint was seen to be dissolved into the film, as shown in Fig. 6(c). The two-dimensional temperature distribution shown in Fig. 6(d) was obtained for the laminate film peeled off the paper module. Higher-temperature portions corresponded to regions with a higher loading of blackbody paint. This paint probably caused the higher temperatures at the regions with poor laminate bonding, since blackbody paint dissolved into the laminate was assumed to lead to greater temperature increases than the blackbody paint attached to the paper module surface. In comparison to the black body paint on the paper surface, the blackbody paint dissolved into the film may absorb light more easily, due to the omnidirectional incidence inside the film. A further reason for the higher temperatures detected at the poor bonding regions may be the air trapped in these areas acting as a resistance, which reflects thermal waves back to the surface.

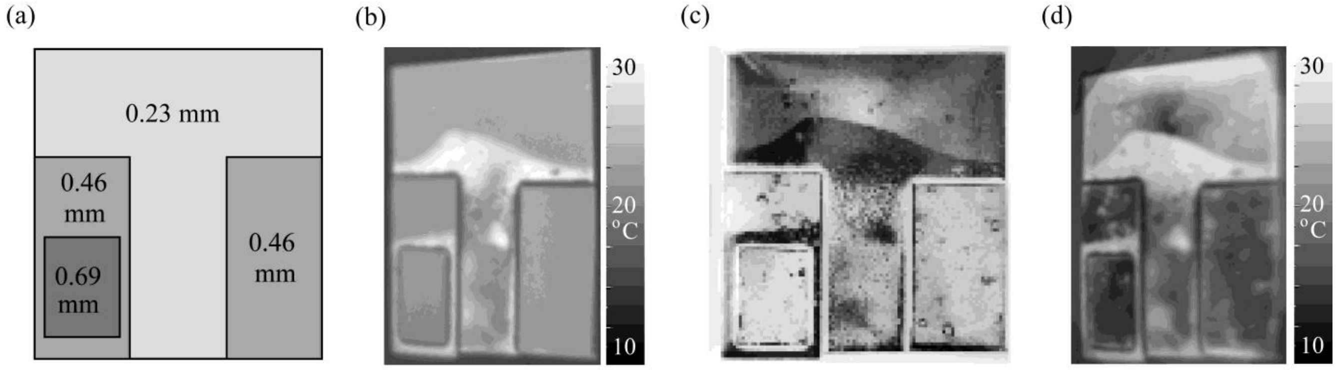

Fig. 6 Analysis of a portion with poor adhesion. (a) Shape of the paper module. (b) Two-dimensional temperature distribution of the surface of the test piece. (c) A photograph of the laminate film peeled off from the paper module. (d) Two-dimensional temperature distribution of the surface of the laminate film peeled off from the paper module.

C. Scope of Application

Colored paper modules (red, green, and blue) were used to test the abilities of the system without blackbody paint. The temperature distributions of the test piece surfaces are shown in Fig. 7, recorded 0.1 s after flash heating. The paper thickness W_p was 0.08 mm, the laminate thickness W_f was 0.09 mm, and the gap thickness W_c was 0.08 mm. The temperature data were converted by the emissivity 0.94, because the emissivities of the colored papers are unknown. The temperature of the test piece was higher than the ambient temperature, and the transmittance of the film covering the cavities resulted in a lower temperature at the region of poor bonding than in the rest of the test piece. Although the detection sensitivity of the system was not good, the cavities were detectable without the use of blackbody paint. These low detection sensitivities are due to the higher reflectivities of the colored papers, compared to that of the blackbody paint (6%). In general, the reflectivities of the colored papers were at least 50% [34], and resulted in the reflection of a substantial portion of the flash. Detection was not achieved with the previous experiment's white colored paper, which exhibited a surface temperature increase of less than 1 ℃ following flash heating. This lack of detection was due to the high reflectivity of the white paper, which is at least 70%.

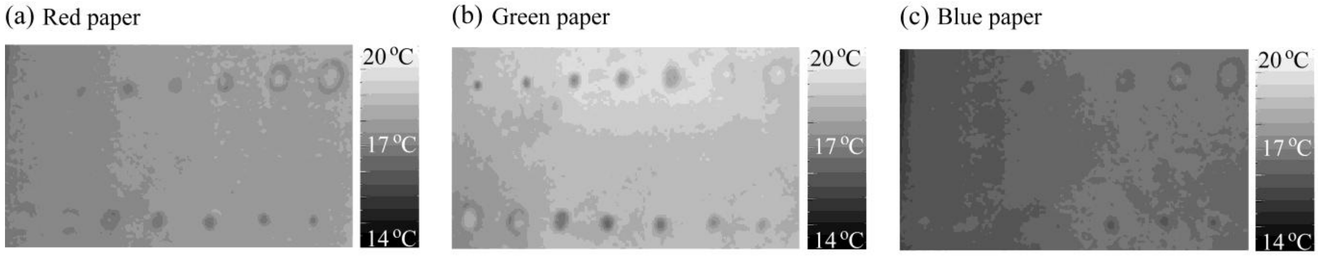

Fig. 7 Temperature distributions of the colored paper modules

The combination of different colored papers into one paper module makes the detection of poor bonding difficult due to the different reflectivities of the paper. In this case, the temperature distribution must be compared with a standard sample that contains no instances of poor bonding. The applicability of the technique may be enhanced by using image processing software.

V. CONCLUSIONS

A method of detecting poor bonding between a laminate and paper surface was described. In this method, rapid heating of the surface of the laminate film bonded to paper by a light flash was followed by thermographic observation of the dynamic changes in surface temperature. The method successfully indicated the presence of regions of poor bonding larger than 1 mm in diameter by the local variations in the rate of cooling. Temperatures in the regions of poor bonding were lower than those in regions of good bonding. This was caused by the low infrared transmissivity of the laminate covering the cavity.

The method was also able to distinguish regions of poor bonding, where the blackbody paint melted into the laminate film. The temperature in these regions was greater than that in the regions of good bonding. This was explained as follows: the blackbody paint that dissolved into the laminate led to a greater temperature increase than the blackbody paint attached to the paper module surface.

The detection method is also capable of detecting instances of poor bonding on colored paper. However, the high reflectivity of white paper prevented the cavities from being measured. Mixing various colors in one sample makes detection more difficult, although use of the method in conjunction with image processing software may broaden its applicability.

ACKNOWLEDGMENT

This work was supported by the Ministry of Education, Culture, Sports, Science and Technology of Japan (MEXT)/Japan Society for the Promotion of Science (JSPS) KAKENHI Grant Number 23560056.

REFERENCES

[1] B. H. Gregory, *Extrusion Coating, Lamination and coextrusion: The Complete process manual*, Bristol, UK: Plastics Information Direct, 2012.

[2] W. Fung, *Coated and laminated textiles*, New York, USA: CRC Press, 2002.

[3] F. Hensen, *Plastics extrusion technology*, 2nd ed., Ohio, USA: Hanser-Gardner, 1997.

[4] E. F. J. Ring, and K. Ammer, "Infrared thermal imaging in medicine," *Physiologial Measurement*, vol. 33, R33–46, March 2012.

[5] M. A. Omar, and A. Zhou, "Dynamic-template processing for passive thermograms: Applied to automotive stamping split-detection," *Elsevier NDT & E International*, vol. 41(8), pp. 582-588, December 2008.

[6] S. Starman, and M. Vaclav, "Automated system for crack detection using infrared thermographic testing," in *Proc. 17th World Conference on Nondestructive Testing*, Shanghai, China, October 25-28 2008.

[7] E. Barreira, and V. P. Freitas, "Evaluation of building materials using infrared thermography," *Elsevier Construction and Building Materials*, vol. 21(1), pp. 218-224, January 2007.

[8] B. Oswald-Tranta, "Thermo-inductive crack detection," *Nondestructive Testing and Evaluation*, vol. 22(2-3), pp. 137-153, June 2007.

[9] W. T. Kim, M. Y. Choi, and J. H. Park, "NDT analysis of metal materials with internal defects using active infrared thermography method," *Key Engineering Materials*, vols. 321-323, pp. 835-840, October 2006.

[10] Y. T. Lo, and K. T. W. Choi, "Building defects diagnosis by infrared thermography," *Structural Survey*, vol. 22(5), pp. 259-263, December 2004.

[11] W. Walter, R.S. Sebastian, W. P. Hans, K. Burkhard, and J. Tino, "Infrared thermography as a non-invasive application for medical diagnostic," in *Proc. XVII IMEKO World Congress*, Dubrovnik, Croatia, June 22-27 2003.

[12] A. C. Legrand, F. Meriaudeau, and P. Gorria, "Active infrared non-destructive testing for glue occlusion detection within plastic lids," *Elsevier NDT&E International*, vol. 35(3), pp. 177-187, April 2002.

[13] G. M. Giovanni, and M. Carosena, "Comparison between thermographic techniques for frescoes NDT," *Elsevier NDT&E International*, vol. 35(8), pp. 559-565, December 2002.

[14] C. A. Balaras, and A. A. Argiriou, "Infrared thermography for building diagnostics," *Elsevier Energy and Buildings*, vol. 34(2), pp. 171-183, February 2002.

[15] W. N. Reynolds, "Thermographic methods applied to industrial materials," *Canadian Journal of Physics*, vol. 64(9), pp. 1150-1154, September 1986.

[16] K. Atsumi, *Medical thermography*, Tokyo, Japan: University of Tokyo Press, 1973.

[17] J. Gershon-Cohen, "Short history of medical thermometry," *Annals of the New York Academy of Sciences*, vol. 121, pp. 4-11, October 1964.

[18] L. D. Favro, X. Han, Z. Ouyang, G. Sun, H. Sui, and R. L. Thomas, "Thomas. Infrared imaging of defects heated by a sonic pulse," *Review of Scientific Instruments*, vol. 71(6), pp. 2418-2421, Jun 2000.

[19] S. E. Burrows, S. Dixon, S. G. Pickering, T. Li, and D. P. Almond, "Thermographic detection of surface-breaking defects using a scanning laser source," *Elsevier NDT&E International*, vol. 44(7), pp. 589-596, November 2011.

[20] T. Li, D. P. Almond, and D. A. S. Rees, "Crack imaging by scanning pulsed laser spot thermography," *Elsevier NDT&E International*, vol. 44(2), pp. 216-225, March 2011.

[21] G. Zenzinger, J. Bamberg, W. Satzger, and V. Carl, “Thermographic crack detection by eddy current excitation,” *Nondestructive Testing and Evaluation*, vol. 22(2-3), pp. 101-111, June 2007.

[22] S. M. Shepard, Y. Hou, T. Ahmed, and J. R. Lhota, “Reference-free interpretation of flash thermography data,” *Insight Non-Destructive Testing and Condition Monitoring*, vol. 48(5), pp. 298-301, May 2006.

[23] J. Sembach, D. Wu, A. Salerno, G. Hora, and G. Busse, “Nondestructive evaluation of delaminations in laminated wood-based panels by thermographical inspection tools,” in *Proc. Workshop on Nondestructive Testing of Panel Products*, Llandudno, UK, October 9-11 1997.

[24] P. Meinlschmidt, and J. Sembach, “Industrial thermographic inspection of delaminations in laminated wood-based panels,” in *Proc. Third European Panel Products Symposium*, Llandudno, UK, October 6-8 1999.

[25] X. Han, L. D. Favro, S. Ouyang, and R. L. Thomas, “Thermosonics: Detecting cracks and adhesion defects using ultrasonic excitation and infrared imaging,” *Journal of Adhesion*, vol. 76(2), pp. 151-162, September 2001.

[26] X. Han, L. D. Favro, S. Ouyang, and R. L. Thomas, “Thermosonics: Detecting cracks and adhesion defects using ultrasonic excitation and infrared imaging,” *Journal of Adhesion*, vol. 76(2), pp. 151-162, September 2001.

[27] P. Meinlschmidt, “Thermographic detection of defects in wood and wood-based materials,” in *Proc. 14th International Symposium of Nondestructive Testing of Wood*, Hannover, Germany, May 2-4 2005.

[28] C. Thiemann, M. F. Zaeh, C. Srajbr, and S. Boehm, “Automated defect detection in large-scale bonded parts by active thermography,” in *Proc. 10th International Conference on Quantitative Infrared Thermography*, Québec, Canada, June 27-30 2010.

[29] C. A. Parker, *Photoluminescence of solutions*, Amsterdam, The Netherlands: Elsevier, 1968.

[30] J. F. Rabek, *Experimental methods in photochemistry and photophysics*, Chichester, UK: Wiley, 1982.

[31] J. C. Scaiano, *Handbook of organic photochemistry Vol. 1*, Boca Raton, USA: CRC Press, 1989.

[32] M. Sugioka, and T. Tsuchibuchi, *Investigation of deterioration for UV irradiated film: Color measurement and haze measurement*, Shimadzu Application News, A345, 2011.

[33] L. Coltro, and J, Borghetti, “Plastic packages for personal care products: Evaluation of Light Barrier Properties,” *Polímeros: Ciência e Tecnologia*, vol. 17, pp. 56-61, 2007.

[34] A. Bejan, and A. D. Kraus, “Heat transfer handbook,” New York, USA: John Wiley & Sons, 2003.

Minoru Aoyagi was born in Tochigi, Japan, on March 31, 1961. He received his B.E. (Electronic Engineering) from the Tokyo University of Agriculture and Technology, Tokyo, Japan, in 1998, and his Ph.D. (Engineering) from the University of Tokyo, Tokyo, Japan, in 1998.

He is currently a Professor in the Electrical and Electronic Department of Nippon Institute of Technology. His previous research includes analysis of semiconductor devices, development of nanomaterials, and development of electric circuits.

Prof. Aoyagi is a member of the Japan Society of Applied Physics, the Institute of Electronics, Information and Communication Engineers of Japan and the Institute of Electrical and Electronics Engineers.

Takefumi Hiraguri was born in Nagano, Japan, on August 18, 1972. He received his M.E. and Ph.D. degree from the University of Tsukuba, Ibaraki, Japan, in 1999 and 2008, respectively.

He is currently an associate professor in the Electrical and Electronic Department of the Nippon Institute of Technology. His main interest is the research and development of MAC protocols for high speed and high communication quality in wireless LANs systems.

Prof. Hiraguri is a member of the Institute of Electronics, Information and Communication Engineers of Japan and the Institute of Electrical and Electronics Engineers.

Takahiro Ueno was born in Saitama, Japan, on March 15, 1970. He received his B.E. and M.E. (Electrical Engineering) from the Nippon Institute of Technology, Saitama, Japan, in 1992 and 1994, respectively, and his Ph.D. (Engineering) from Keio University, Yokohama, Japan, in 2002.

He is currently an associate professor in the Electrical and Electronic Department of the Nippon Institute of Technology. His main research interest is in electrical sliding contacts, including the influence of atmospheric conditions on sliding contacts and the sliding characteristics of a pantograph slider.

Prof. Ueno is a member of the Institute of Electronics, Information and Communication Engineers of Japan, the Institute of Electrical Engineers of Japan and the Institute of Electrical and Electronics Engineers.